Magnetic Resonance Imaging of Blood Flow with a Phase Subtraction Technique

In Vitro and In Vivo Validation

AVERY J. EVANS, MD,* FUMIHARU IWAI, MD,† THOMAS A. GRIST, MD,‡ H. DIRK SOSTMAN, MD,* LAURENCE W. HEDLUND, PHD,* CHARLES E. SPRITZER, MD,* ROSA NEGRO-VILAR, MA,* CRAIG A. BEAM, PHD,* AND NORBERT J. PELC, SCD§

Evans AJ, Iwai F, Grist TA, Sostman HD, Hedlund LW, Spritzer CE, Negro-Vilar R, Beam CA, Pelc NJ. Magnetic resonance imaging of blood flow with a phase subtraction technique: in vitro and in vivo validation. Invest Radiol 1993;28: 109–115.

RATIONALE AND OBJECTIVES. **One promising approach to flow quantification uses the velocity-dependent phase change of moving protons. A velocity-encoding phase subtraction technique was used to measure the velocity and flow rate of fluid flow in a phantom and blood flow in volunteers.**

METHODS. **In a model, the authors measured constant flow velocities from 0.1 to 270.0 cm/second with an accuracy (95% confidence intervals) of ±12.5 cm/second. There was a linear relationship between the magnetic resonance imaging (MRI) measurement and the actual value (r^2 = .99; P = .0001).**

RESULTS. **Measuring mean pulsatile flow from 125 to 1,900 mL/minute, the accuracy of the MRI pulsatile flow measurements (95% confidence intervals) was ±70 mL/minute. There was a linear relationship between the MRI pulsatile flow measurement and the actual value (r^2 = .99; P = .0001). In 10 normal volunteers, the authors tested the technique in vivo, quantitating flow rates in the pulmonary artery and the aorta. The average difference between the two measurements was 5%. In vivo carotid flow waveforms obtained with MRI agreed well with the shape of corresponding ultrasound Doppler waveforms.**

CONCLUSIONS. **Velocity-encoding phase subtraction MRI bears potential clinical use for the evaluation of blood flow. Potential applications would be in the determination of arterial blood flow to parenchymal organs, the detection and quantification of intra- and extra-cardiac shunts, and the rapid determination of cardiac output and stroke volume.**

KEY WORDS. **Blood flow; magnetic resonance imaging; phase contrast imaging; velocity measurement.**

NONINVASIVE MEASUREMENT OF blood flow velocity has long been a goal of magnetic resonance imaging (MRI) investigation. Even before the development of MRI, several investigators demonstrated that motion affects the MRI signal.[1,2] Various nonimaging and imaging techniques have been devised to measure fluid flow velocity and rate.[3–13]

One promising approach to flow quantification uses the velocity-dependent phase change of moving protons. Carr and Purcell,[14] and later Stejskal,[15] demonstrated that phase shifts occur with motion along a magnetic field gradient. Hahn[16] proposed a spin-echo pulse sequence that would produce a phase shift proportional to the velocity of the moving protons. After the advent of MRI, Moran[17] suggested that these previously described velocity-dependent phase shifts might be used to determine blood flow velocity in humans. O'Donnell[18] proposed a phase-imaging technique, wherein two images are acquired and the difference in images is dependent only on velocity. Wedeen et al[19] and Firmin et al[20] also have implemented phase-imaging techniques.

We have modified the technique proposed by O'Donnell to use a gradient-echo acquisition, thereby increasing the relative signal from blood and reducing image acquisition

From the *Department of Radiology, Duke University Medical Center, Durham, North Carolina, the †Department of Surgery, Keio University Hospital, Tokyo, Japan, the ‡Department of Radiology, University of Wisconsin Hospital, Madison, Wisconsin, and the §Department of Radiology, Stanford University School of Medicine, Stanford, California.

Reprint requests: Avery J. Evans, MD, Box 3808, Department of Radiology, Duke University Medical Center, Durham, NC 27710.

Received March 4, 1992, and accepted for publication, after revision, September 1, 1992.

time, thus improving its clinical usefulness. A preliminary report has been written concerning the clinical usefulness of this method for determining vessel patency and flow direction.[21] Caputo et al[22] measured flow with this technique in the pulmonary arteries and with steady flow in a phantom. However, the accuracy of this method for measuring pulsatile flow rate has not been established. The purpose of this work is to determine the accuracy of this technique in the measurement of steady flow velocities and pulsatile flow rates (both mean and instantaneous) in a phantom, and to apply the technique to a small number of normal volunteers.

According to the technique proposed by O'Donnell,[18] the velocity of a flowing fluid can be measured by acquiring two views per phase-encoding step. The phase difference ($\Delta\Phi$) between the two resulting images is: $\Delta\Phi = \gamma\Delta m\nu$, where Δm is the change in the gradient's first moment (with respect to time) due to the modified bipolar pulse, ν is the velocity, and γ is the gyromagnetic ratio. The moment is calculated by integrating the gradient pulse shape and timing with respect to time. Thus, the phase difference between the two images for any given pixel is related directly to flow velocity along the axis of the applied bipolar pulse. The phase portion of an MRI is dependent not only on velocity, but also on many other parameters, including magnetic field inhomogeneity, eddy currents, radio frequency penetration effects, and details of pulse sequence timing. Acquiring two images that differ only in the first moment of the gradient waveform in the direction of interest allows the subtraction of these effects and produces an image dependent only on motion in the encoded direction.[21] In the current study, flow in the slice-encoding direction was measured.

To encode velocity, the change in the first moment of the selectable gradient is adjusted so that all velocities in a predetermined range produce phase shifts between π and $-\pi$ radians of phase. For instance, if the limit is set at 100 cm/second, then velocities between -100 and $+100$ cm/second produce linear phase shifts between $-\pi$ and π radians. The stronger the change in the first moment, the greater the phase change per change in velocity, and the smaller the range of velocities that can be encoded. Any velocities outside the selected range will be improperly represented. This misrepresentation has been termed "aliasing," and can lead to inaccurate velocity measurement.

Materials and Methods

A phantom was constructed consisting of Plexiglas tubes of different diameters joined in series so that the same volume of fluid passed through each tube (Fig. 1). The tubes were circular in cross-section with inner diameters of 19.05, 15.85, and 12.70 mm (±.05 mm). The flow direction in each tube was parallel to the axis of the magnet bore. The Plexiglas tubes were joined with sufficient length of Tygon tubing in between the tubes to ensure that the fluid had regained full transverse magnetization (5 × T1 weight) before reentering the imaging plane. The fluid used in these experiments was distilled water doped with gadolinium chloride-EDTA, giving a T1 weight of 580 mseconds (±80 mseconds).

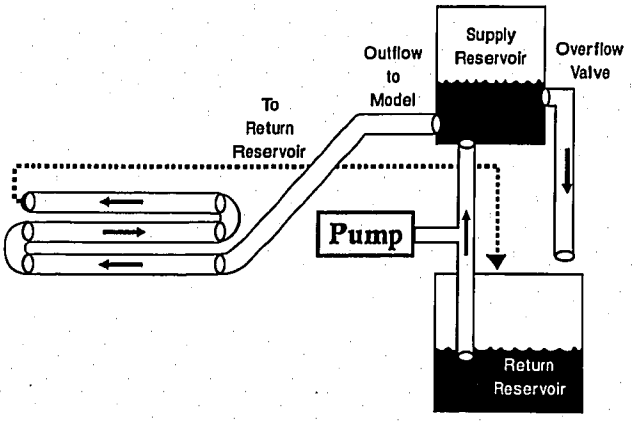

Fig. 1. Diagram of the apparatus that produced the steady flow. A 25-L gravity feed tank supplied fluid to the tubes. A return reservoir collected the outflow of the tubes. A centrifugal pump returned the fluid to the gravity feed tank. The overflow valve on the feed tank maintained a constant fluid level in the feed tank.

Flow Production: Steady Flow

The apparatus for producing steady flow is shown schematically in Figure 1. A 25-L gravity feed tank suspended 3 m above the magnet bore supplied fluid to the tubes. A return reservoir collected the outflow of the tubes. A centrifugal pump recycled the fluid from the return reservoir to the gravity feed tank. An overflow valve on the feed tank maintained a constant fluid level in the feed tank, draining excess fluid back to the return tank. At all times, the outflow of the pump exceeded the outflow from the model, so that the fluid level in the feed tank was maintained at a constant level, ensuring an unchanging pressure head and therefore constant flow in the tubes. The flow rate was adjusted by a valve between the supply reservoir and the phantom.

Flow rates were measured (±3%) by timing the filling of a graduated cylinder and averaging multiple measurements. Mean flow velocities were calculated by dividing the flow rate (cm^3/second) by the cross-sectional area of the tube (cm^2) to obtain the mean velocity (cm/second). Mean flow constant velocities ranged from 0.1 to 270.0 cm/second.

Pulsatile Flow

Pulsatile flow was generated by a pump that has been previously described.[23] Mean pulsatile flow rates varied from 125 to 1,900 mL/minute. Mean pulsatile flow rates were measured (±3%) by timing the filling of a graduated cylinder and averaging multiple measurements. To validate the MRI measurements, instantaneous pulsatile flow rates (mL/minute) were measured (±8%) with a Transonics flow meter and clamp-on flow probe (Transonics, Ithaca NY). The frequency ("heart rate") of the pump was set at 60 beats/minute.

Patients

After obtaining informed consent, 10 normal volunteers with no history of cardiac disease were imaged. Ages ranged from 22 to 42 years.

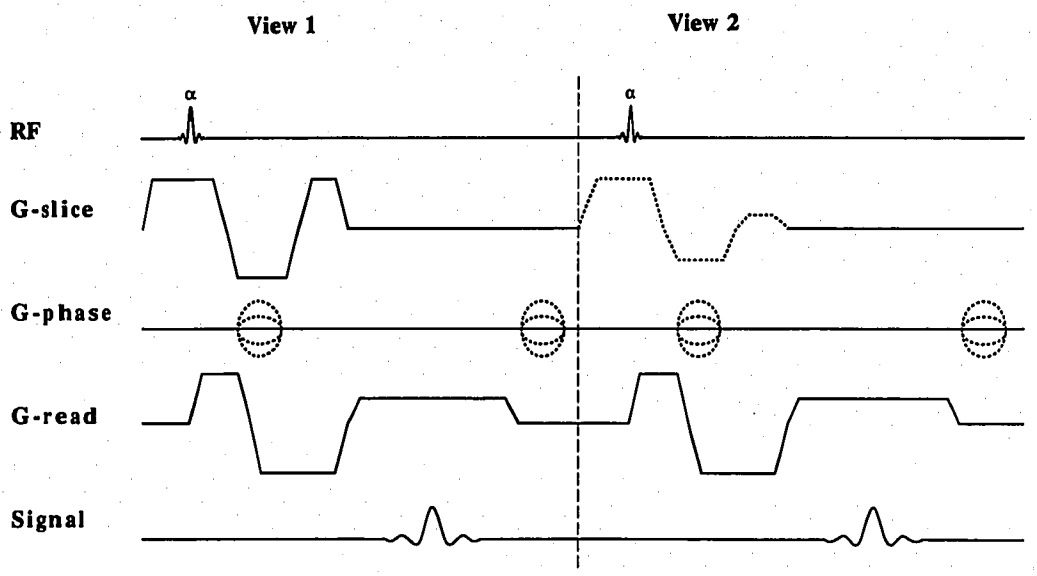

Fig. 2. Schematic representation of the pulse sequence diagram. The selectable flow-encoding gradient is shown on all three axises, but in practice may be used on one, two, or all three orthogonal dimensions. RF: radio frequency.

Magnetic Resonance Imaging Parameters

All imaging was performed on a 1.5-Tesla GE Signa system (GE, Milwaukee, WI). For the steady-flow experiments, all imaging was in the axial plane; 10-mm–thick slices; 30° flip angle; TR/TE, 33/13 mseconds; and matrix, 256 × 128 pixels. A two-excitation scan was acquired in less than 13 seconds. The velocity-encoding gradient was set at a level approximately 25% higher than the expected highest flow velocity. The pulse sequence diagram is shown in Figure 2.

For the pulsatile flow and human experiments, imaging was performed in the cine mode, with the same imaging parameters as the steady flow experiments. Axial imaging planes were used for measuring carotid flow. In the main pulmonary artery and aorta, oblique planes perpendicular to the direction of flow were prescribed using an initial set of spin-echo images. Temporal resolution varied according to the heart rate of the patient, and averaged approximately 16 frames per second. A two-excitation scan was acquired in the time of 256 heart beats.

MRIs were analyzed using a computerized vascular analysis program, Velcalc (GE, Milwaukee, WI). Circular regions of interest were placed in the lumens of the vessels to include as much of the lumen of the vessel as possible, without averaging in portions of the wall.

Ultrasound Imaging

Pulsatile flow waveforms in the carotids were obtained with an Acuson 128 computed sonographic device with Doppler capability.

Statistical Methods

The strength of a linear relationship between the MRI flow measurements and the actual flow in vitro, and aortic versus pulmonary artery measurements in vivo, was measured with Pearson product moment correlation.

To obtain an estimate of the potential error in the MRI flow measurement, the method of least squares was used to fit MRI flow measurements to the flow measurements from the graduated cylinder. Each of these equations was inverted to yield 95% confidence interval estimates on the actual value given a particular MRI value, using the method given by Fleiss.[24]

Results

The relationship between the actual constant flow velocity and the velocity measured by the MRI phase subtraction technique for the three different tubes is shown in Figure 3. Over a range of physiologic velocities, linear regression analysis demonstrates a correlation coefficient (r^2 = .99; P = .0001). To obtain an estimate of the potential error in the MRI flow measurement, the method of least squares was used to fit MRI flow measurements to the flow measurements from the graduated cylinder (see Materials and Methods section). The 95% confidence interval estimates using this method predict an approximate accuracy of ±12.5 cm/second for MRI measurements of constant flow over the range of velocities studied (which includes values higher than those seen in normal blood vessels).

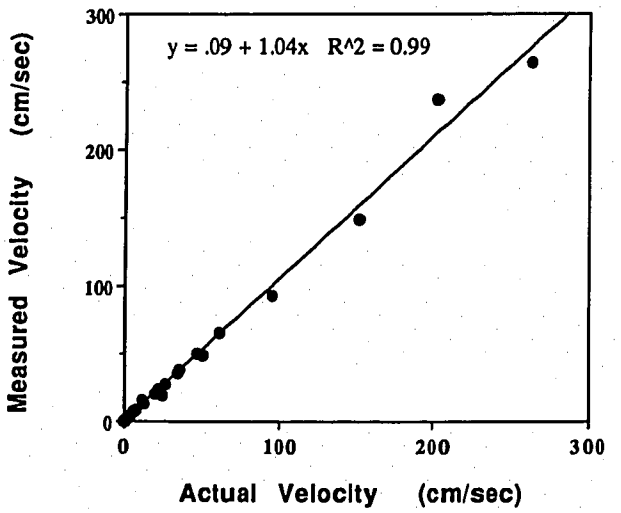

Fig. 3. Measured versus actual velocity for steady flow in all three tubes (19.05, 15.85, and 12.70 mm). Velocities ranged from 0.1 to 270 cm/second.

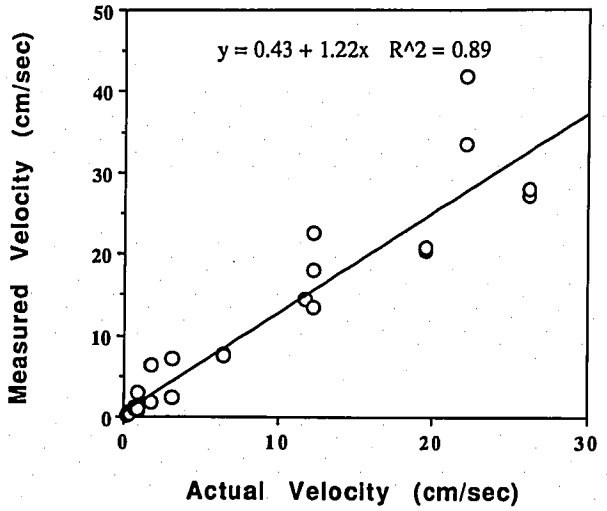

Fig. 4. Demonstration of the effect of setting the selectable gradient at a much higher maximum velocity than actually occurred. In this experiment, the flow-encoding gradient was set at a level at least 30 times higher than the actual maximum flow velocity. Measured versus actual velocity for the largest diameter tube (19.05 mm).

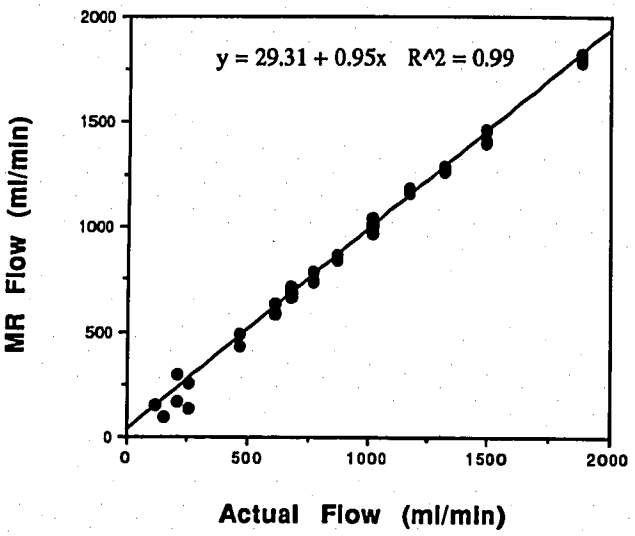

Fig. 6. The mean pulsatile flow measurements in milliliters per minute are represented. Mean volumes ranged from 125 to 1,900 mL/minute. Peak instantaneous velocities ranged from −25 to greater than 300 cm/second. Data from the three different tube diameters are combined. MR: magnetic resonance.

Figure 4 shows the effect of setting the selectable gradient at a much higher maximum velocity than the flow velocity that actually occurred. In this experiment, the flow-encoding gradient was set at a level at least 30 times higher than the actual maximum flow velocity. (Low velocity flows were examined because it is not possible to set the flow-encoding gradient higher than 1,000 cm/second). Measurements were made in the largest diameter tube (19.05 mm). As might be expected, there is increased scatter. The correlation between the actual and the measured velocities is not as well described with a linear regression (r^2 = .89).

When the selectable-encoding gradient is set at the value less than the actual flow velocity in the vessel, there is essentially no correlation between the measured and the actual velocity (Fig. 5). This phenomenon has been termed "aliasing."

The results from the pulsatile flow measurements are shown in Figure 6. Mean pulsatile flow in milliliters per minute (determined by averaging measurements in a graduated cylinder) is compared with mean pulsatile flow rate measured with the MRI method. Mean flow rates ranged

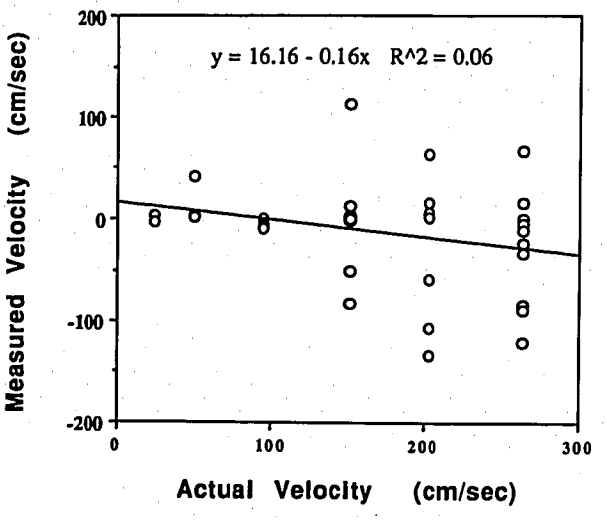

Fig. 5. Data collected with the selectable encoding gradient set at a value less than the actual flow velocity in the vessel Measured versus actual velocity in the smallest diameter tube (12.70 mm) with velocities ranging from 10 to 270 cm/second.

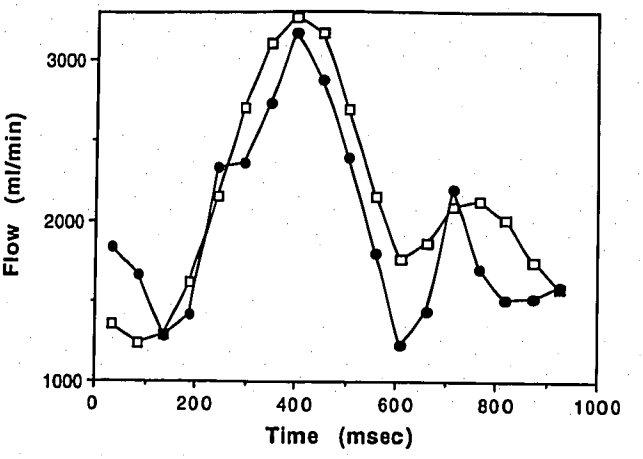

Fig. 7. Instantaneous flow in the phantom as measured with the ultrsonic flow probe (solid circles) and the magnetic resonance imaging technique (open squares).

from approximately 125 to 1,900 mL/minute. Velocities ranged from approximately −25 to more than 300 cm/second (peak aortic flow velocity = 100–150 cm/second). Data from the three different tube diameters are combined. The y-intercept is 29.31 mL/minute (not statistically different from 0). There was a linear relationship between the two measurements (r^2 = .99; P = .0001). Again, the method of least squares was used to obtain an estimate of the potential error in the MRI pulsatile flow measurement. The 95% confidence interval of the MRI flow rate estimate is ±70 mL/minute.

Measurements of different pulsatile flow waveforms measured with ultrasound and MRI are shown in Figure 7. Qualitatively, the MRI pulsatile flow waveforms compare well with those determined by the ultrasonic flow probe.

In vivo pulsatile waveforms from the internal and external carotid arteries of a normal volunteer are demonstrated in Figure 8. The ultrasound waveforms have been plotted with the same number of points as the MRI waveforms to present a more effective comparison. The shapes of the MRI pulsatile flow waveforms are similar to the shapes of the ultrasound pulsatile flow waveforms.

A comparison of mean aortic and pulmonary flow rates in 10 normal volunteers is demonstrated in Figure 9. There is a linear relationship between the two measurements (r^2 = .95; P = .01). The average difference between the two measurements was 5%.

A representative sample of aortic and pulmonary pulsatile flow waveforms from one of the normal volunteers is shown in Figure 10 (the difference in flow in this case was 6%).

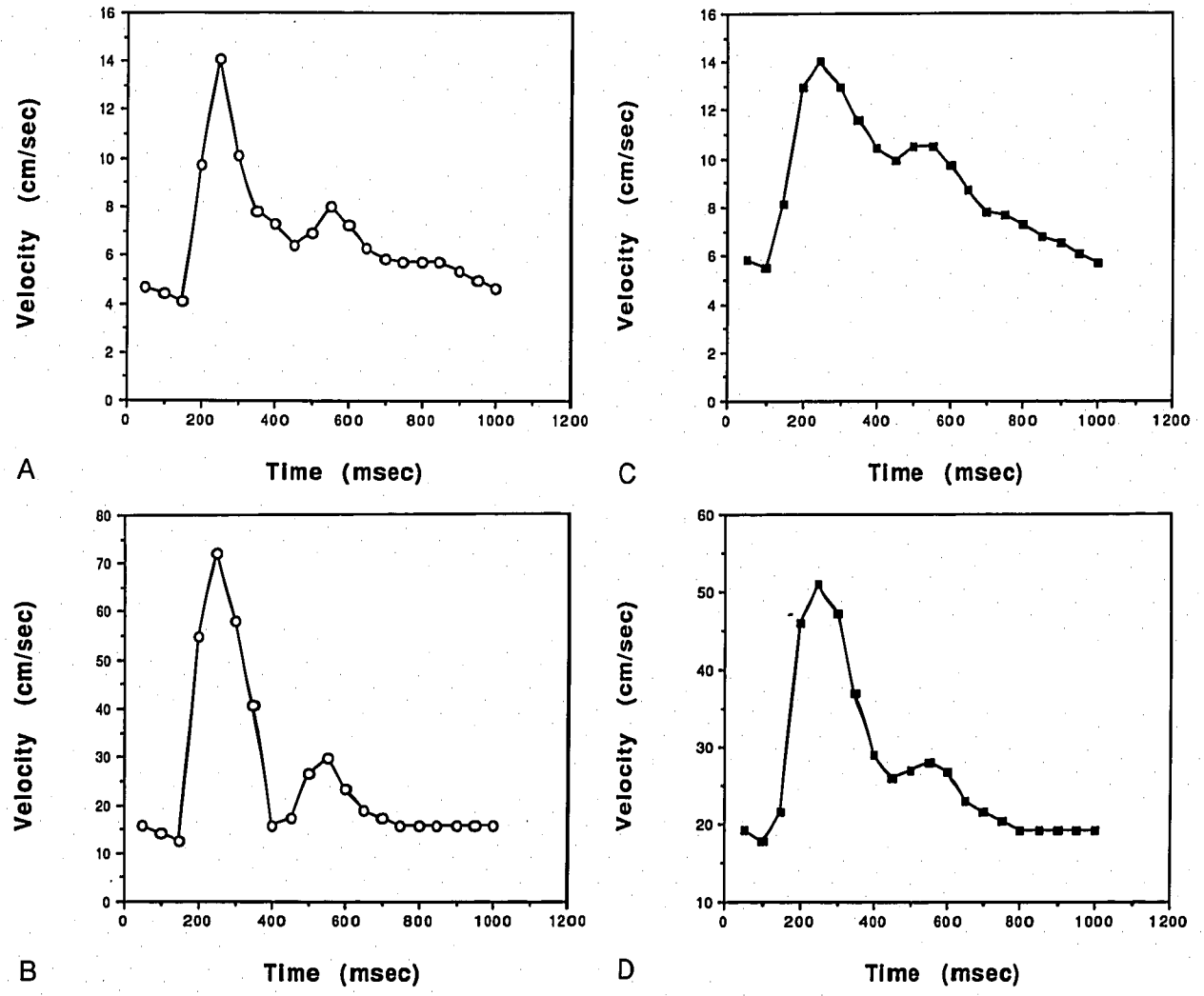

Figs. 8A–8D. (A) Magnetic resonance imaging measurement of instantaneous flow velocity in the external carotid artery of a normal volunteer. (B) Ultrasound measurement of instantaneous flow velocity in the external carotid artery of a normal volunteer. (C) Magnetic resonance imaging measurement of instantaneous flow velocity in the internal carotid artery of a normal volunteer. (D) Ultrasound measurement of instantaneous flow velocity in the internal carotid artery of a normal volunteer.

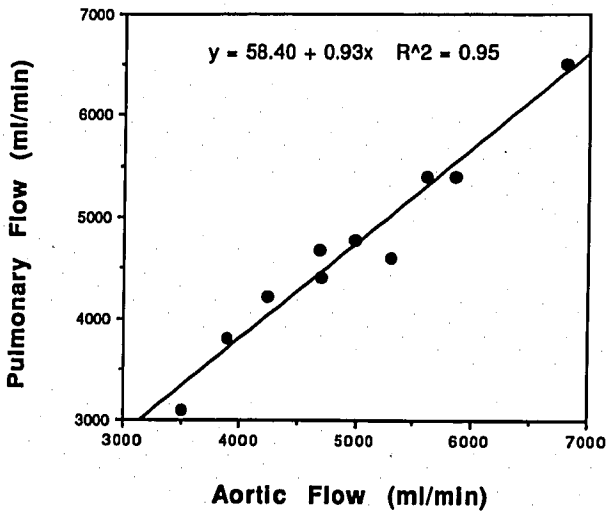

Fig. 9. Correlation of magnetic resonance imaging measurement of mean flow volume (mL/minute) in the pulmonary artery and the aorta of 10 normal volunteers.

Discussion

This study examined the accuracy of measurements of constant and pulsatile flow velocity using a phase subtraction technique. For constant flow (Fig. 3), the potential error in the MRI flow measurement (95% confidence interval) was ±12.5 cm/second.

As demonstrated in Figures 3 to 5, the selectable flow-encoding strength should be set appropriately for the velocity of the expected flow to reach optimal accuracy and precision. If the selectable flow-encoding gradient is set at a level much higher than the actual flow, the precision of the flow measurement is then degraded. Our results suggest that a value approximately 25% higher than the peak expected flow is adequate, while allowing room for error if the actual flow is higher. On the other hand, as demonstrated in Figure 5, it is more important to be certain that the selected encoded velocity range is set at a level that is higher than the peak actual velocity. Failure to do so will result in gross inaccuracy of a flow measurement. In most clinical situations, it should be possible to anticipate the highest flow velocities and to set the encoded velocity appropriately.

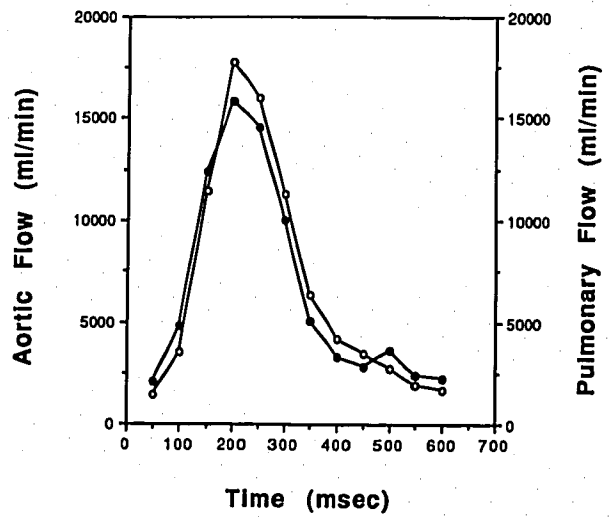

Fig. 10. A representative sample of aortic and pulmonary pulsatile flow waveforms from one of the normal volunteers (the difference in flow in this case was 6%). Magnetic resonance imaging measurement of instantaneous flow volume (mL/minute) in the pulmonary artery (solid circles) and the aorta (open circles).

For pulsatile flow, like steady flow, there is a linear relationship between the MRI measurements and the actual flow rate (r^2 = .99; P = .0001). The 95% confidence interval of the MRI flow rate estimate is ±70 mL/minute.

This technique can, like ultrasound, depict pulsatile flow waveforms (Fig. 8). Potentially, these MRI pulsatile flow waveforms are clinically useful. Ultrasound pulsatile flow waveforms have been used as indicators of the resistance to flow in a vessel.[25] In general, the higher the resistance in a vessel, the lower the diastolic flow. For example, external carotid artery resistance to flow is known to be higher than the resistance to flow in the internal carotid artery. The MRI pulsatile flow waveform from a normal volunteer correlates with the ultrasound in showing a higher diastolic flow (Fig. 9).

Although the ultrasound and the MRI carotid flow waveforms are similar in shape, the ultrasound velocities are much higher. Most likely, this occurs for two reasons. First, the ultrasound measures the peak flow in the center of the vessel (the highest velocities being in the center), whereas the MRI measures the mean flow across the entire circumference of the vessel. Second, there is a distribution of velocities even in the center of the vessel, and the ultrasound measures the highest of these, whereas the MRI measurement averages these velocities.

In 10 normal volunteers, the measured aortic and pulmonary flow rates had a mean difference of 5% (Fig. 9), suggesting that this technique can produce accurate flow measurements in vivo. In the normal volunteers, aortic flow averaged 5% greater than pulmonary flow. Recent measurements in animals indicate that bronchial circulation is 0.5% to 1.5% of cardiac output.[26] This small difference is unlikely to account for the difference we observed. However, a 3.5% to 4.5% difference is well within the experimental error of the technique. The errors that may occur using this technique have been described by others. According to these authors, only small errors occur with changes in scan parameters such as TR, TE, and flip angle, but larger errors can occur when adjusting other factors such as zero velocity (background), pixel value, and the maximum and minimum encoded velocity values.[27,28] Buonocore and Bogren[28] discuss these factors in detail in their recent work.

In summary, this technique combines the multiplanar im-

aging capability of conventional MRI with the ability to acquire—in the same image—accurate information about fluid flow rate and velocity. Potential applications for this technique would be in the determination of arterial blood flow to parenchymal organs, the detection and quantification of intra- and extra-cardiac shunts, and the rapid determination of cardiac output and stroke volume.

References

1. Suryan G. Nuclear resonance in flowing liquids. Proc Indian Acad Sci [Am] 1951;33:107–111.
2. Hahn EL. Spin echoes. Phys Rev 1958;80:580–594.
3. Singer J. Blood flow rates by nuclear magnetic resonance measurements. Science 1959;130:1652–1653.
4. Hahn EL. Detection of sea-water motion by nuclear precession. J Geophys Res 1960;65:776–777.
5. Morse OC, Singer JR. Blood velocity measurements in intact subjects. Science 1970;170:440–441.
6. Grover T, Singer JR. NMR: spin echo flow measurements. J Appl Phys 1971;42:938–940.
7. Jones DW, Child TF. NMR in flowing systems. In: Waugh JJ, ed. Advances in magnetic resonance. New York, NY: Academic Press; 1976:123–148.
8. Singer JR. NMR diffusion and flow measurements and an introduction to spin phase graphing. J Phys E 1978;11:281–291.
9. Halbach RE, Battocletti JH, Salles-Cunha SX, Sances A. The NMR blood flowmeter—design. Med Phys 1981;8:444–451.
10. Salles-Cunha SX, Halbach RE, Battocletti JH, Sances A. The NMR blood flowmeter—applications. Med Phys 1981;8:452–458.
11. Battiocletti JH. Blood flow measurement by NMR. Crit Rev Biomed Eng 1986;13:311–367.
12. Axel L. Blood flow effects in magnetic resonance imaging. AJR 1984; 143:1157–1166.
13. Haacke EM, Smith AS, Lin W, Lewin JS, Finelli DA, Duerk JL. Velocity quantification in magnetic resonance imaging. Top Magn Reson Imaging 1991;3(3):34–49.
14. Carr H, Purcell E. Effects of diffusion on free precession in nuclear magnetic resonance experiments. Phys Rev 1954;94:630–638.
15. Stejskal EO. Use of echoes in a pulsed magnetic-field gradient to study anisotropic, restricted diffusion and flow. J Chem Phys 1965; 43:3597–3603.
16. Hahn EL. Detection of sea-water motion by nuclear precession. J Geophys Res 1960;65:776–777.
17. Moran PR. A flow zeugmatographic interlace for NMR imaging in humans. Magn Reson Imaging 1982;1:197–203.
18. O'Donnell M. NMR blood flow imaging using multiecho, phase contrast sequences. Med Phys 1985;12(1):59–64.
19. Wedeen V, Rosen B, Chesler D, Brady T. MR velocity imaging by phase display. J Comput Assist Tomogr 1985;9:530–536.
20. Firmin DN, Nayler GL, Klipstein RH, Underwood SR, Rees RSO, Longmore DB. In vivo validation of MR velocity imaging. J Comput Assist Tomogr 1987;11(5):751–756.
21. Spritzer CE, Pelc NJ, Lee JN, Evans AJ, Sostman HD, Riederer SJ. Preliminary experience with rapid MR blood flow imaging using a phase sensitive limited flip angle gradient refocused pulse sequence. Radiology 1990;176(1):256–261.
22. Caputo GR, Kondo C, Masui T, Geraci SJ, Foster EI, O'Sullivan MM, Higgins CB. Right and left lung perfusion: in vitro and in vivo validation with oblique-angle, velocity-encoded cine MR imaging. Radiology 1991;180:693–698.
23. Evans AJ, Hedlund LW, Herfkens RJ. A cardiac phantom and pulsatile flow pump for magnetic resonance imaging studies. Invest Radiol 1988;23(8):579–583.
24. Fleiss JL. The design and analysis of clinical experiments. New York, NY: John Wiley and Sons; 1984:41–43.
25. Grant EG, Tessler FN, Perrella RR. Clinical Doppler imaging. AJR 1989;152:707–717.
26. Mango MG, Fishman AP. Origin, distribution and blood flow of bronchial circulation in anesthetized sheep. J Appl Physiol 1982; 53:272–279.
27. Sommer G, Noorbehesht B, Pelc N, et al. Normal renal blood flow measurement using phase-contrast cine magnetic resonance imaging. Invest Radiol 1992;27:465–470.
28. Buonocore MH, Bogren H. Factors influencing the accuracy and precision of velocity-encolded phase imaging. Magn Reson Med 1992; 26:141–154.

Announcements

8th Annual San Diego Postgraduate Magnetic Resonance Imaging Course, March 8–12, 1993, Hotel Del Coronado, San Diego, California. Sponsored by the Department of Radiology, University of California, San Diego School of Medicine. Credit: 29 Category 1 AMA hours. Fee: physician $595, (after February 23) $645; resident, fellow, nurse, technologist $425, (after February 23) $475. Contact: Dawne Ryals, Ryals and Associates, PO Box 1925, Roswell, GA 30077-1925; call 404-641-9773, or fax 404-552-9859.

PET and SPECT Imaging of Living Brain Chemistry, March 10—12, 1993, Thomas B. Turner Building, Johns Hopkins Medical Institutions, Baltimore, Maryland. Sponsored by Johns Hopkins University School of Medicine. Credit: 18 AMA Category 1 hours. Fee: $495, physicians; $395, residents, fellows, and allied health physicians. Contact: Patty Campbell, Johns Hopkins Medical Institutions, Office of Continuing Education, Turner Bldg, 720 Rutland Ave., Baltimore, MD 21205; call 410-955-6046.

Focus on Hemodialysis Access: Creation, Maintenance, and Salvage, March 13, 1993, Le Meridien, San Diego at Coronado, California. Sponsored by the Office of Continuing Medical Education, the University of California, San Diego School of Medicine. Credit: 6.5 Category 1 hours. Fee: $75. Contact: Conference Management Associates, P.O. Box 2586, La Jolla, CA 92038; call 619-454-3212.

7th Annual Magnetic Resonance Imaging Conference, March 14–17, 1993, Arizona Biltmore Resort Hotel, Phoenix, Arizona. Sponsored by Barrow Neurological Institute of St. Joseph's Hospital and Medical Center. Credit: Category I credit. Contact: Maria Sodaro, RN, BSN, Research and Education Coordinator, Radiologic Education Center, St. Joseph's Hospital and Medical Center, 350 W. Thomas Road, Phoenix, AZ 85013; call 602-285-3956.